The Paleoenvironment and Lithic Taphonomy of Shi'Bat Dihya 1, a Middle Paleolithic Site in Wadi Surdud, Yemen

Luca Sitzia, Pascal Bertran, Stéphane Boulogne, Michel Brenet, Rémy Crassard, Anne Delagnes, Marine Frouin, Christine Hatté, Jacques Jaubert, Lamya Khalidi, et al.

Research Article

The Paleoenvironment and Lithic Taphonomy of Shi'Bat Dihya 1, a Middle Paleolithic Site in Wadi Surdud, Yemen

Luca Sitzia,[1,*] Pascal Bertran,[1,2] Stéphane Boulogne,[2] Michel Brenet,[1,2] Rémy Crassard,[3] Anne Delagnes,[1] Marine Frouin,[4,5] Christine Hatté,[6] Jacques Jaubert,[1] Lamya Khalidi,[7] Erwan Messager,[8,9] Norbert Mercier,[5] Alain Meunier,[4] Stéphane Peigné,[10] Alain Queffelec,[1] Chantal Tribolo,[5] and Roberto Macchiarelli[4,8]

[1]PACEA, UMR 5199 CNRS, Université de Bordeaux 1, Talence, France
[2]INRAP, Pessac, France
[3]Archéorient, UMR 5133 CNRS, Maison de l'Orient et de la Méditerranée, Lyon, France
[4]Département Géosciences, Université de Poitiers, Poitiers, France
[5]CRPAA-IRAMAT, UMR 5060 CNRS, Université de Bordeaux 3, Pessac, France
[6]Laboratoire des Sciences du Climat et de l'Environnement, Domaine du CNRS, Gif-sur-Yvette, France
[7]Consejo Superior de Investigaciones Científicas, Institución Milá Y Fontanals, C/Egipcíaques, Spain
[8]Département de Préhistoire, UMR 7194 CNRS, Muséum National d'Histoire Naturelle, Paris, France
[9]CEPAM UMR 7264 CNRS, Campus Saint Jean d'Angély, Nice, France
[10]Département Histoire de la Terre, UMR 7207 CNRS, Muséum National d'Histoire Naturelle, Paris, France

Correspondence
*Corresponding author;
E-mail: ca3bigio@gmail.com

Received
16 March 2012
Accepted
6 July 2012

Scientific editing by Jamie Woodward

Published online in Wiley Online Library (wileyonlinelibrary.com).

doi 10.1002/gea.21419

The Shi'bat Dihya 1 site in western Yemen, dated by optically stimulated luminescence to 55 ka, provides insight into the Middle Paleolithic peopling of the Arabian Peninsula. The archaeological layer is interstratified within thick, sandy silt floodplain deposits filling a piedmont basin. Luminescence dates, lack of soil development, and gypsum precipitation indicate a high accretion rate of the floodplain during Marine Isotope Stage 3, in connection with a (semi)-arid environment. Rapid overbank sedimentation was likely a result of the remobilization of loess material deposited on the Yemeni Great Escarpment at the periphery of the adjacent Tihama coastal sand desert or of other sources. Fabric and size analyses of the lithic artifacts, together with spatial projections, indicate site modifications by floods. Primary modifications include (1) selective accumulation of medium-sized lithic pieces as a result of hydraulic sorting, (2) bimodal orientation of artifacts, and (3) ripple-like arrangement of lithics and bone/tooth fragments. The overrepresentation of teeth may also be a consequence of sorting. Although floods have distorted the original site patterning, long-distance transport of artifacts by water can be excluded, as indicated by relatively high refitting rate, close proximity of artifacts derived from the same block of raw material, and lack of abrasion of the pieces. Therefore, the site is considered "geologically" *in situ* because its remobilization by water occurred shortly after human abandonment. This study also stresses that the effective preservation of a site cannot be assessed without careful taphonomic study, even in a potentially favorable depositional context such as silty alluvium.

INTRODUCTION

The Middle Paleolithic site of Shi'bat Dihya 1 (SD1) in western Yemen (Figure 1A) is one of the oldest human occupations in the Arabian Peninsula preserved in stratigraphic context. Discovered as part of research activities in Wadi Surdud by the Paleo-Y international project (Macchiarelli and Peigné, 2006; Macchiarelli, 2009) and dated by optically stimulated luminescence (OSL) at approximately 55 ka (Delagnes et al., 2012), the site has yielded a rich Middle Paleolithic lithic industry accompanied by a small number of faunal remains. Thus, SD1, which is part of a larger complex of prehistoric sites, is an important reference point for understanding human population

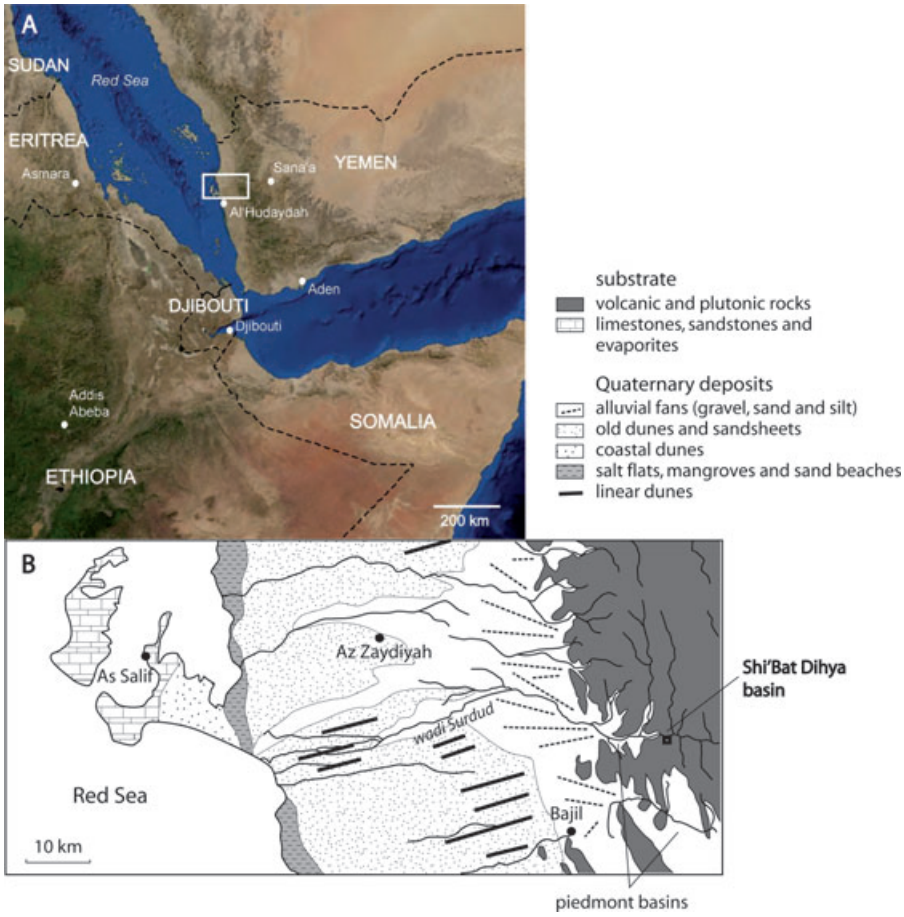

Figure 1 Study area. (A) Satellite picture of the Arabian Peninsula (ESRI World Imagery Basemap Data). The rectangle indicates the location of Figure 1B. (B) A schematic geological map of the area (modified from Munro and Wilkinson, 2007) and site location.

dynamics across the Arabian Peninsula during the Upper Pleistocene.

SD1 is located in the first low hills of the Great escarpment of Yemen, approximately 15 km east of the city of Bajil (N15°11.371′, E43°25.670′; Figure 1B). This area of foothills, at the junction between the highlands and the coastal plain, has a high potential for the preservation of Upper Pleistocene archaeological and paleoenvironmental records. The archaeological layer of SD1 is preserved in a sedimentary sequence composed primarily of sandy silt, which fills a small Quaternary tectonic basin cut by the Wadi Surdud and its tributaries. This sediment is connected downstream to large Pleistocene alluvial cones distributed throughout the piedmont and the coastal plain (Munro and Wilkinson, 2007). The general stratigraphy of the fill has been compiled from various sections that are visible along the Wadi Surdud and the Shi'Bat Dihya and Al Sharj gullies. Correlations among these sections have been established based on elevation data and the main calcrete units (MCU), which can be readily traced across the landscape.

This article has two aims: (1) to characterize in detail the paleoenvironmental context of the Paleolithic occupation of SD1, as limited data are currently available to document Marine Isotope Stage (MIS) 3 in the Arabian Peninsula, and (2) to assess the preservation of the site to highlight any possible distortions in the archaeological record. Although the archaeological level SD1 is interbedded in a fine-grained alluvial sequence, thereby favoring the preservation of artifacts and their organization, flooding may have influenced the integrity of the site. The taphonomic study was primarily based on a geoarchaeological approach. The hypothesis of a redistribution of the artifacts by river flows was assessed using three methods: fabric analysis, which is designed to test the existence of preferred orientations of artifacts (Bertran and Texier, 1995; Lenoble and Bertran, 2004); particle size analysis, used to evaluate the hydraulic sorting of artifacts (Schick,

1986; Bertran et al., 2006); and spatial analysis of the distribution of lithic and faunal remains. The results were then compared with data from the archaeological study to develop the most likely scenario for the taphonomic history of the site.

METHODS

Sediments

For the sedimentological and pedological characterization of the alluvial stratigraphic sequence, field observations were supplemented by sedimentological and geochemical analyses. Seventeen samples were taken for grain size analysis at PACEA laboratory, University of Bordeaux. After treatment with hydrogen peroxide (H_2O_2) to remove organic matter and with formic acid (HCOOH, diluted) to remove secondary calcium carbonate, the samples were analyzed by sieving the fraction greater than 63 μm and using laser granulometry (Mastersizer S Malvern, Marlvern, Worcestershire, UK) for the fraction below 63 μm. Forty-one samples were prepared for calcium carbonate ($CaCO_3$), total organic carbon (TOC), and nitrogen (N) measurements according to the procedure proposed by Gauthier and Hatté (2008). The samples were combusted in a Fisons Instrument NA 1500 Element Analyzer and the carbon content determined with Eager software. A standard was inserted every 10 samples. Inorganic carbon content in bulk sediment was calculated assuming that mineral carbon exists only as $CaCO_3$. Carbon isotopic signature was measured with a continuous flow EA-IRMS by coupling a Fisons Instrument NA 1500 Element Analyzer to a ThermoFinigan Delta + XP Isotope-Ratio Mass Spectrometer. Two home internal standards (oxalic acid, $\delta^{13}C = -19.31‰$ and GCL, $\delta^{13}C = -26.70‰$) were inserted every eight samples. Results are reported in the δ notation: $\delta^{13}C = (R_{sample}/R_{standard} - 1) \times 1000$, where R_{sample} and $R_{standard}$ are the $^{13}C/^{12}C$ ratios of the sample and the international standard Vienna Pee Dee Belemnite Standard (VPDB), respectively. Measurements were at least trebled to ensure representativeness. Extreme values were twice checked. Twelve thin sections were cut from blocks impregnated under vacuum with a polyester resin according to the protocol described by Guilloré (1980). Raman spectroscopy was used to determine certain mineral phases observed in the thin sections. The spectra acquisition was performed at CRPAA, University of Bordeaux, using a Renishaw RM2000 – Leica DMLM and determined using the RRUFF database (Downs, 2006). The X-ray diffraction (XRD) patterns were recorded at HYDRASA, University of Poitiers, using a PANanalytical Xpert Pro diffractometer with Ni-filtered Cu-Kα radiation generated at 40 kV and 40 mA and step size of 0.017°2θ. XRD diffractograms were recorded in the 2–65 and 2–34 ° 2θ Cu Kα angular ranges for random powders and oriented mounts, respectively. The determination of the clay species was performed using the decomposition procedure recommended by Lanson (1997) and the calculated XRD patterns using NEWMOD software (Reynolds, 1985). Phytolith extractions from bulk samples were made using standard methods but failed to provide any result, either because of preservation issues of biogenic silica in sandy sediments or low phytolith production in the local environment.

Taphonomy

Lithic pieces with a long (a) axis (i.e., the maximum dimension in any plane) greater than 2 cm and all faunal remains were located in three dimensions with an infrared theodolite, and then numbered. Lithic pieces less than 2 cm in length were collected within each 25 cm quadrant area and then sieved under water on a 2 mm mesh.

The orientation and the dip of 228 objects were measured using a compass and an inclinometer. The calculation of eigenvalues and the projections on a Schmidt diagram were performed with the program Stereo32, version 6.3.3 (Allmendinger, 2005). The isotropy index (SI = E3/E1) and the elongation index (EL = 1 – (E2/E1)) were calculated according to Benn (1994). The intensity of the preferred orientation (Vector Magnitude L) and the *p*-value of the Rayleigh test, which tests whether the preferred orientation is significant, were calculated using the method proposed by Curray (1956).

The particle width (i.e., the particle intermediate b-axis) of all the lithic artifacts collected was also quantified. For each square, the pieces smaller than 2 cm collected during the excavation and the refuse from the 2 mm water sieving were passed through the following series of screens: 2, 4, 5, 10, 20, 31.5, and 50 mm. Lithics longer than 2 cm were divided into size classes by passing them individually through the diagonal of the mesh of a sieve to avoid damaging of the edges and to ensure the correspondence of the widths measured by the caliper and by sieving. The width of the pieces passing through a mesh sieve d = *a* mm is approximately w = $a\sqrt{2}$ mm (Bertran et al., 2006). The mesh sieves used in the present study correspond to true widths of artifacts, respectively, equal to 2.8, 5.7, 7.1, 14.1, 28.3, 44.5, and 70.7 mm. The total number of lithics measured was 26,729 (Table I). These data were compared to the results of three experimental series made by one of us (M.B.) from blocks of rhyolite collected near the site in the Shi'Bat Dihya gully. The blocks have the same petrographic characteristics as

Table I Particle size of the archaeological (SD1) and the experimental assemblages. The sizes of each class are given in the number of elements.

	Size classes (mm)							
	2–4	4–5	5–10	10–31.5	20–31.5	31.5–50	>50	*N*
				SD1 archaeological assemblage				
Full assemblage	5513	4195	9181	5232	1992	613	3	26,729
B19	0	0	1	3	1	0	0	5
C15	14	12	47	39	21	8	0	141
D14	72	60	127	85	35	10	0	389
D15	44	75	133	125	67	26	0	470
D16	468	450	892	1923	1017	312	2	5064
D17	540	323	662	278	53	23	0	1879
D18	380	243	629	197	42	9	0	1500
D19	202	185	494	258	100	18	0	1257
D20	75	69	169	84	36	6	0	439
E13	0	0	3	4	5	1	0	13
E14	108	149	273	135	53	30	0	748
E15	351	228	464	183	78	33	0	1337
E16	529	409	929	265	56	12	0	2200
E17	272	283	678	390	99	25	1	1748
E18	284	193	371	199	80	32	0	1159
E19	364	294	532	243	66	9	0	1508
E20	97	96	210	111	33	14	0	561
F15	175	112	280	154	65	16	0	802
F16	251	179	370	148	74	26	0	1048
F17	281	206	493	113	7	3	0	1103
F18	343	190	405	80	3	0	0	1021
F19	533	337	735	141	1	0	0	1747
F20	130	102	284	74	0	0	0	590
				Experimental debitage				
Total	1444	211	267	120	45	38	2	2127
Block 1	490	72	75	32	19	19	1	708
Block 2	460	76	101	50	11	9	0	707
Block 3	494	63	91	38	15	10	1	712

those found within the archaeological layer. The core reduction strategies adopted for the experiment reproduced those observed at SD1 (Delagnes et al., 2012). These core reduction strategies used a Levallois unidirectional flaking method in order to obtain elongated, triangular flakes and a laminar volumetric unidirectional method for producing pointed blades. The hammerstones were two rhyolite pebbles that were also collected in the vicinity of the site. The percussion was direct and tangential, and the preparation of the striking platform was performed using the same hammerstone. After each experimental production episode all debitage was collected and measured by sieving in the same manner as the archaeological series (Table I).

Projections of the artifacts on the horizontal (XY) and vertical (YZ) planes were performed to document the spatial configuration of the site. Seven distinct groups of pieces showing the same physical characteristics and assumed to derive from the same initial block of rhyolite were identified, and the rate of refitting corresponding to each block was calculated.

RESULTS

Sedimentary Context

Two main alluvial units separated by a major erosional unconformity have been recognized in the Wadi Surdud Formation filling the Shi'Bat Dihya basin (Figures 2, 3). The lower unit, called the Al Sharj Member after the local name of a gully along which it outcrops, is preserved in the form of alluvial remnants against the slopes (Figure 4). Following our preliminary fieldwork, this unit has yielded only a few scattered lithic artifacts, and has been dated to approximately 85 ka (MIS 5) by OSL on quartz grains (Table II). The upper unit, or Shi'Bat Dihya Member, truncates the previous formation and overlaps it. This unit constitutes a 30-m-thick sequence

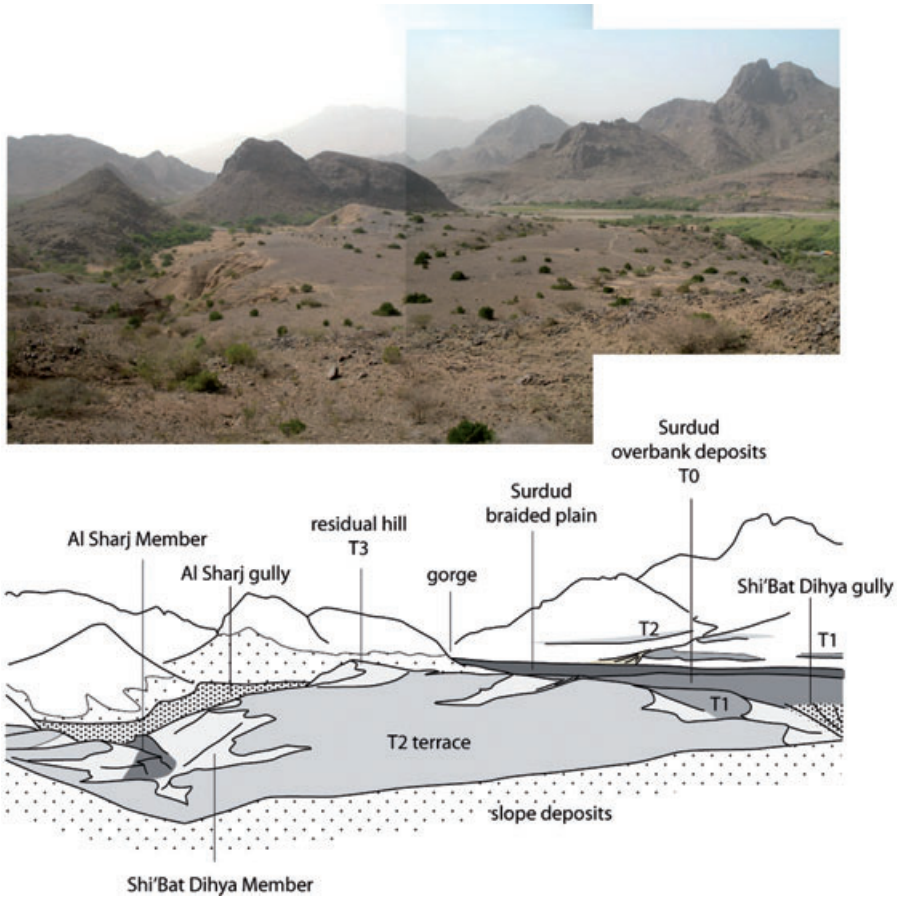

Figure 2 General overview of the basin of Shi'Bat Dihya and interpretation.

preserved over 0.1 km^2 on the left bank of Wadi Surdud. All dates obtained in this member range between 63 and 42 ka, demonstrating that it coincides with the first part of MIS 3.

The archaeological deposit forms a thin layer of artifacts in the lower part of the Shi'Bat Dihya Member. The stratigraphy recorded at the site, on the north bank of Shi'Bat Dihya gully, shows two lithostratigraphic units (Figure 5). The first unit (1.5 m thick) forms a large lens composed of pluridecimetric to decimetric horizontal beds of medium- to fine-grained sands (Figure 6). The second unit (4.5 m thick) is formed by the alternation of horizontal decimetric to pluridecimetric layers of carbonate-rich fine sands to coarse silts ($0.1\% < CaCO_3 < 8.4\%$; Figure 7) and weakly organic (clayey) silts ($0.02\% < TOC < 0.11\%$). The C:N ratio remains under 5.6 all along the sequence, while the $\delta^{13}C$ values range between −20.51 and −23.46‰, with a mean of *ca.* −21‰. A few small lenses of sand and small, angular gravel from the slope are locally interstratified in the sequence. A 30-cm-thick discontinuous calcrete horizon occurs at the top of the lower unit. Carbonated nodules are equally dispersed through the entire sequence. The clay minerals, highly homogenous, are largely dominated by disordered mixed-layer illite/smectite (I/S) that are smectite-rich (S = 70–80%). The clays also include, in small quantities, ordered mixed-layer I/S with 90–95% illite in addition to mica, chlorite, and kaolinite. From powder data, the minerals identified by XRD include quartz, feldspar, gypsum, and halite. The lower unit is interpreted as deposits from secondary channels or crevasse splays, whereas the upper unit, which contains the archaeological layer SD1, corresponds to flood deposits over an alluvial plain (Reineck and Singh, 1975; Miall, 1996).

The upper part of the sequence, visible along the south bank of Shi'Bat Dihya gully and along Al Sharj gully (Figure 5), is also composed of sandy deposits from crevasse splays or secondary channels interstratified with floodplain silts. In the latter, the stratification becomes indistinct and reflects hyperconcentrated flows, which are associated with a high silt load in suspension (Pierson and Costa, 1987; Li et al., 1997; Xu, 1998). Several levels of

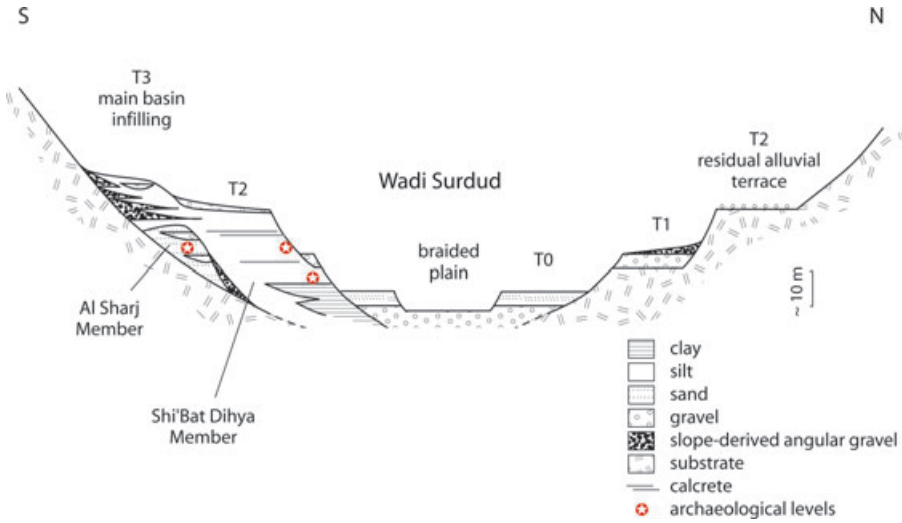

Figure 3 Schematic stratigraphy of the basin fill of Shi'Bat Dihya (Wadi Surdud Formation) and location of the archaeological finds.

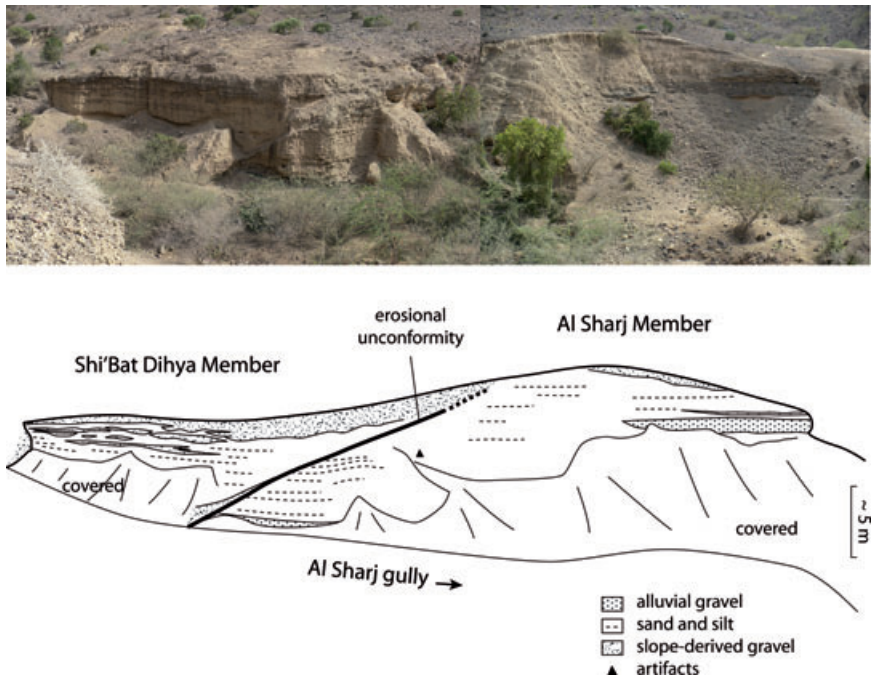

Figure 4 View of the Al Sharj Member and interpretation.

continuous calcrete are also present (Figure 8). The top of the sequence is capped by a desert pavement of iron-crusted cobble gravels.

The field observations show that no mature soil characterized by well-differentiated horizons is present in the studied sequence, although pedological changes are visible at the microscopic level. Bioturbation is moderate and has not completely destroyed the original depositional features (Figure 9A). Vertical transfers of clayey silts and organic matter are locally visible (Figure 9B). The poor sorting of the illuviated particles suggests that illuviation occurred rapidly, either during floods or in conjunction with rainfall on bare ground (Courty and Fédoroff, 1985). The presence of fragments of depositional surface crusts (Valentin and Bresson, 1992) in the matrix of the sediment confirms that, at least seasonally, the ground was bare of vegetation.

In the biological pores (biogalleries), gypsum occurs occasionally through the whole sequence in the form of lenticular crystals (Porta and Herrero, 1990; Figure 9C). The nature of this mineral was confirmed using Raman analysis. The absence of gypsum-bearing formations in

Table II Dose rates, equivalent doses (De), and ages. The samples are ordered by stratigraphic order.

			Dose rates (Gy/ka)										Equivalent doses (Gy/ka)		Ages (ka)	
Sample	Member	Profile	Beta	±	Alpha	±	Gamma	±	Cosmic	±	Total	±		±		±
AS1–08/OSL2	Shi Bat Dihya	3	1.343	0.148	0.078	0.024	0.739	0.055	0.130	0.017	2.29	0.16	96.4	3.9	**42**	4
AS1–08/OSL3	Shi Bat Dihya	3	1.422	0.154	0.088	0.026	0.790	0.059	0.065	0.009	2.36	0.17	120.2	3.6	**51**	4
SD2–08/OSL8	Shi Bat Dihya	2	1.497	0.165	0.088	0.027	0.801	0.060	0.123	0.016	2.51	0.18	131.1	6.6	**52**	5
SD2–08/OSL7	Shi Bat Dihya	2	1.371	0.154	0.075	0.023	0.724	0.080	0.098	0.013	2.27	0.18	127.1	2.5	**56**	5
SD2–08/OSL6	Shi Bat Dihya	2	1.433	0.162	0.077	0.024	0.727	0.081	0.088	0.011	2.32	0.18	115.4	4.6	**50**	4
SD1–08/OSL19	Shi Bat Dihya	1	1.421	0.160	0.080	0.025	0.849	0.094	0.103	0.013	2.45	0.19	135.4	6.8	**55**	5
SD1–08/OSL10	Shi Bat Dihya	1	1.488	0.159	0.099	0.031	0.684	0.076	0.098	0.013	2.37	0.18	127.5	6.4	**54**	5
SD1–08/OSL11	Shi Bat Dihya	1	1.343	0.145	0.087	0.027	0.774	0.086	0.092	0.012	2.30	0.17	128.3	6.4	**56**	5
SD1–08/OSL18	Shi Bat Dihya	1	1.246	0.132	0.076	0.023	0.724	0.081	0.086	0.011	2.13	0.16	106.6	3.2	**50**	4
SD1–08/OSL17	Shi Bat Dihya	1	1.182	0.127	0.072	0.022	0.754	0.084	0.083	0.011	2.09	0.15	132.2	9.3	**63**	7
SD1–08/OSL12	Shi Bat Dihya	1	1.290	0.134			0.828	0.092	0.079	0.010	2.20	0.16	120.9	6.5	**55**	5
SD1–08/OSL16	Shi Bat Dihya	1	1.103	0.119			0.760	0.085	0.079	0.010	1.94	0.15	94.2	7.5	**49**	5
SD1–08/OSL16 bis	Shi Bat Dihya	1	1.171	0.126			0.760	0.085	0.079	0.010	2.01	0.15	109.8	4.4	**55**	5
SD1–08/OSL15	Shi Bat Dihya	1	1.144	0.120			0.703	0.078	0.079	0.010	1.93	0.14	120.8	3.6	**63**	5
SD1–08/OSL14	Shi Bat Dihya	1	1.125	0.121			0.746	0.083	0.077	0.010	1.95	0.15	111.3	17.8	**57**	10
AS2–08/OSL20b	Al Sharj		1.141	0.122			0.775	0.086	0.105	0.014	2.02	0.15	168.9	15.2	**84**	10

See Figure 5 for profile numbers. The beta and alpha dose rates are deduced from U, Th, and K contents estimated with high-resolution gamma spectrometry. The alpha dose rate is assumed negligible for sandy samples, which were HF treated before De determination. The gamma dose is deduced either from Al2O3 dosimetry when available or from the U, Th, K contents. Alpha, beta, and gamma dose rates take into account the attenuation by water (estimated 10 ± 3% for silty samples, 8 ± 3% for sandy samples). All uncertainties for the dose rates include statistic and systematic sources. The equivalent doses are calculated using the Finite Mixture Model (e.g., Galbraith and Green, 1990) and are presented with their statistical uncertainty only. In order to take into account the uncertainty on the source calibration, a 2% systematic uncertainty was quadratically added to the final age uncertainty.

the drainage basin upstream excludes the hypothesis that gypsum originated from the reworking of older evaporitic rocks. Therefore, the presence of this mineral is probably linked to calcium ions and sulfates brought by wind from the coastal sebkhas. The smectite-rich I/S that dominates the clay minerals and the halite detected by XRD likely have a similar source. Gypsum accumulated in the biological pores, but this phenomenon occurs regularly throughout the sequence without the formation of clearly delineated gypsum horizons. This configuration is consistent with the low occurrence of pedogenic phenomena and suggests that the gypsum is related to either the very early stages of soil formation or the evaporation of a subsurface groundwater rich in calcium and sulfates under (semi)-arid climatic conditions.

Calcitic hypocoatings and micritic impregnations are the dominant crystalline features. The impregnations, 0.1 mm to several centimetres in diameter, have a nodular appearance and grow either in the host matrix or around root voids. The crystalline mass is enriched with Fe hydroxides, and there are well-developed sparite crystals inside the nodules or along the walls of the voids. The continuous calcrete horizons (MCU) are characterized by an abundance of these crystal features, which are similar in their configuration to the microstructure "alpha" described by Wright (2007) in his classification of calcretes. The lack of a pedogenic profile associated with carbonated horizons and the observed micromorphological features suggest that the origin of these features is not related to soil leaching. Instead, the characteristics of the nodules are comparable to the groundwater calcretes described by Mack et al. (2000) and Wright (2007). The formation of nodules thus appears to be caused by carbonate precipitation in the capillary zone and just above the groundwater table in response to conditions of high evaporation. Subsequently, the MCU are interpreted as reflecting relatively long phases of carbonate precipitation in relation to a stable groundwater table close to the ground surface.

Archaeological Context

The total extent of the archaeological layer was estimated at several hundred square meters. The excavated area covered 21 m^2 (Figure 10) and yielded a large lithic assemblage that is assumed to be representative (Delagnes et al., 2012). In all, 5488 lithic pieces longer than 2 cm were found. The lithics recovered from SD1 form a homogeneous assemblage, both technologically and in terms of edge preservation, which is uniform and generally good. Apart from occasional impact damage, the edges are fresh and present no macroscopic traces of natural abrasion. Raw materials are made of five main groups: rhyolite

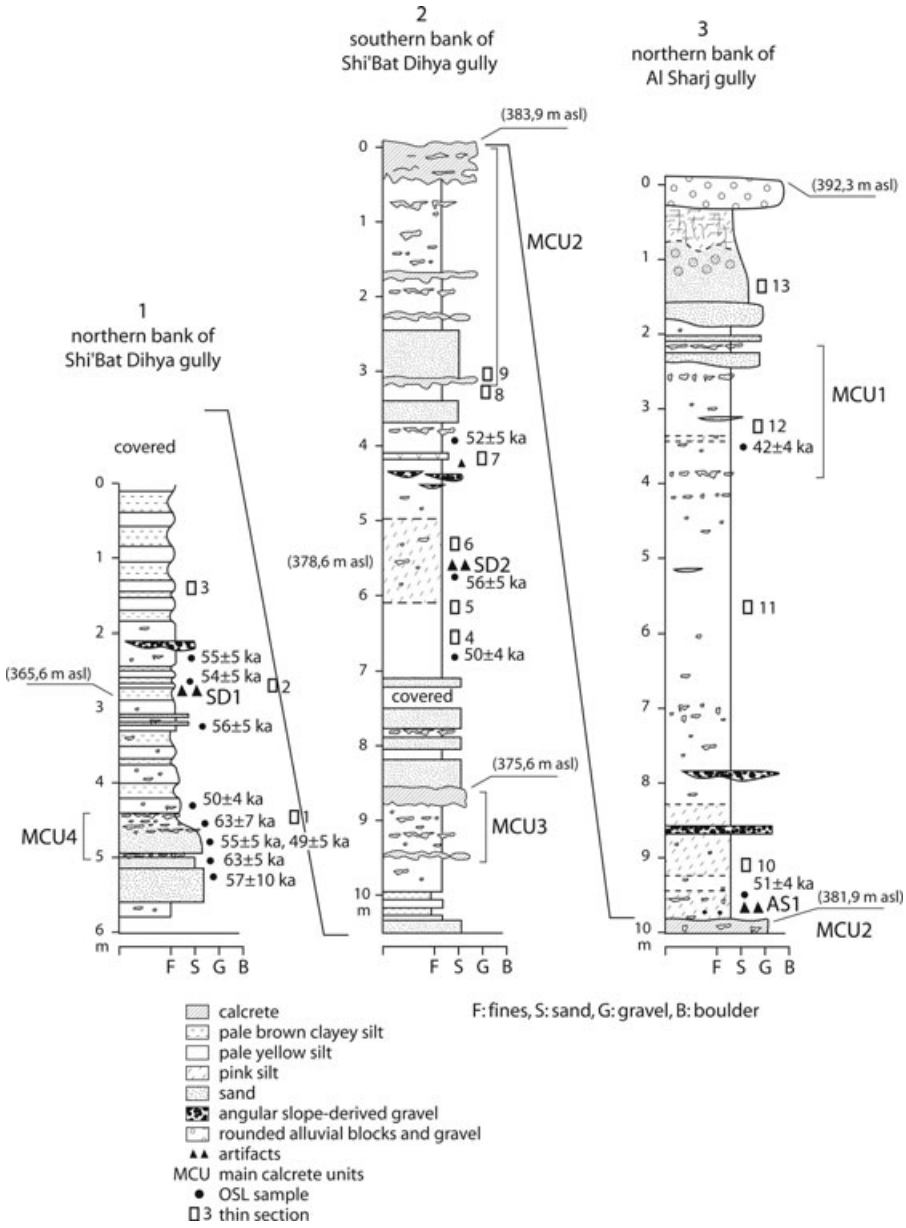

Figure 5 Stratigraphy of the Shi'Bat Dihya Member and position of the archaeological layers, OSL dates, and thin sections.

(93.8%), basalt (2.4%), phonolite (1.8%), quartz (1.7%), and sandstone (0.3%). All of these materials are easily and abundantly accessible in the nearby streambed as well as in the gravel lenses interstratified within the Al Sharj Member. The debitage of rhyolite is characterized by two main core reduction strategies, one producing blades and the other producing pointed flakes, accompanied by a more marginal Levallois production (Table III, Figure 11). Core reduction strategies result in a variety of end products: blades, pointed blades, pointed flakes, and Levallois flakes, with long unmodified cutting edges that were left un-retouched. Retouched pieces are extremely rare ($n = 25$ or 0.5% of the lithics > 2 cm) and, apart from one example, are made exclusively in rhyolite. The association of rhyolite with other significantly less well-represented materials highlights the deliberate exploitation of different local resources to fulfill distinct needs: sandstone and occasionally basalt for hammer stones, simple debitage in phonolite, basalt and quartz, and heavy duty tools in basalt. This pattern suggests that diverse activities took place at SD1 within the context of a habitation site.

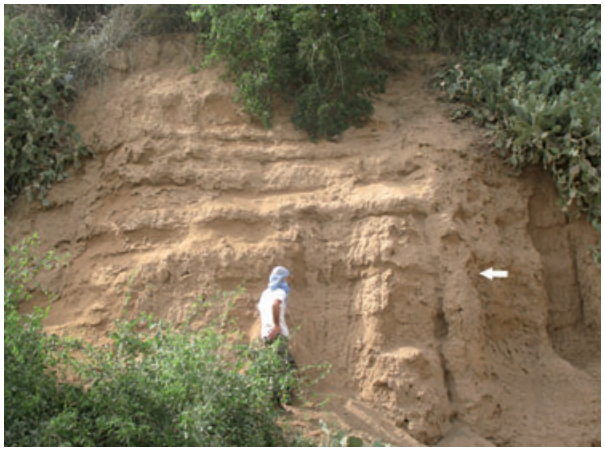

Figure 6 View of the Shi'Bat Dihya Member from the north bank of the small wadi of the same name. The archaeological layer is indicated by an arrow.

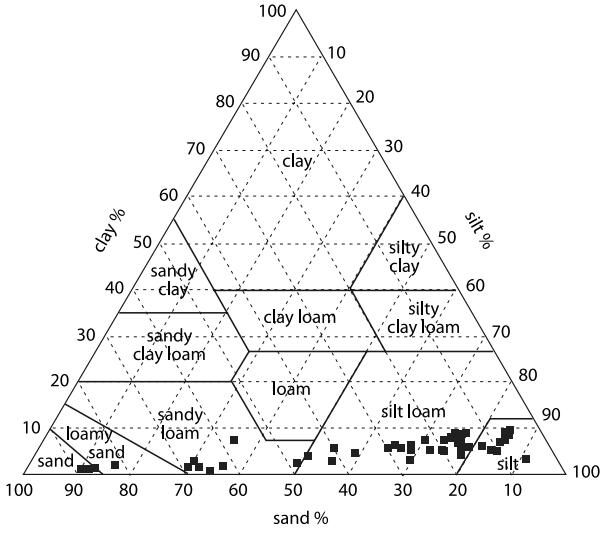

Figure 7 Sediment grain size range of the Shi'Bat Dihya Member on the U.S. Department of Agriculture triangle of textures.

The SD1 lithic assemblage is typically Middle Paleolithic in character. But it differs significantly, both qualitatively and quantitatively, from the late Levantine Mousterian and from the late Middle Stone Age assemblages documented south and north of the Arabian Peninsula *ca.* 60–50 ka. It is assumed that this assemblage reflects an Arabian Middle Paleolithic tradition that emerged and developed locally in this part of the Arabian Peninsula, which maintained locally favorable conditions for long-term human settlements, even during the arid periods of the Upper Pleistocene (Delagnes et al., 2012).

Figure 8 Scattered calcium carbonate nodules (protruding out of the section) in a silty alluvium, merging into a continuous calcrete at the top of the photo (Shi'Bat Dihya Member).

Fabric Types

Within all the squares analyzed, the distribution of the orientations of the major axes of the artifacts is polymodal. However, two modes dominate, which correspond to the directions N 60–70° and N 140–180°. The corresponding rose diagrams are shown on the map of distribution of the lithics (Figure 12).

The Vector Magnitude L for these squares varies within 12–16% (Table IV). To test the hypothesis of bimodality in the distribution of the orientations, the angles were doubled and the Vector Magnitude recalculated. After doubling the angles, L increases to 25–26% for the squares D18 and E16 and to 13% for all measures. In contrast, L decreases for squares D16 and F17–18. For the entire series of measurements, the *p*-values of the Rayleigh test never yields values below the threshold of 0.05, indicating the absence of a significant preferred orientation. Conversely, the *p*-value falls below 0.05 for the overall sample when the angles are doubled (Table IV). The hypothesis of a bimodal distribution of orientations can thus be accepted.

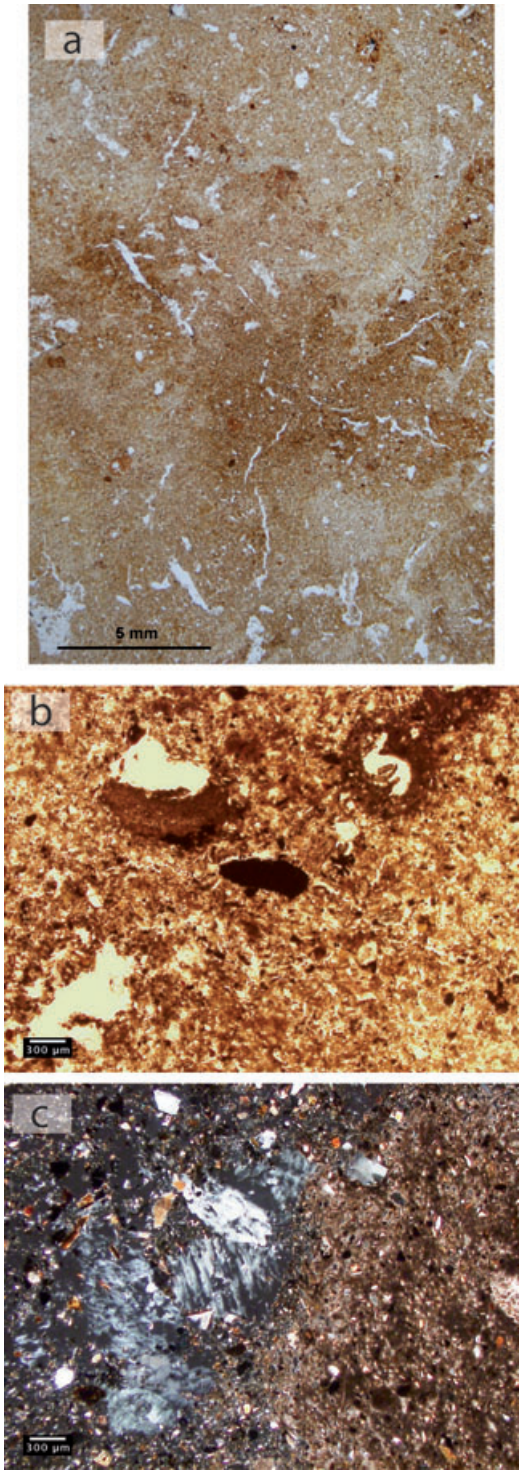

Figure 9 Microscopic thin-sections from Al Sharj Member. (A) Microfacies of floodplain deposits. Bedding (alternating light colored sands and darker silt-dominated layers) is disturbed by bioturbation. Thin section 2 (see location on Figure 4), PPL. (B) Poorly sorted clayey silt coating in a biogallery and micritic nodule. Thin section 1 (see location on Figure 4), PPL. (C) Gypsum crystals in the voids and ferruginous carbonate nodule. Thin section 1 (see location on Figure 4), XPL.

Particle Size Distribution of the Lithics

The particle size distribution of the lithics collected in each square is shown in Figure 13 and 14, and Table I. The results from the entire excavated surface are highly homogeneous. All squares are characterized by a bell-shaped curve approaching a Gaussian distribution, with a mode set in the class of $d = 5$–10 mm (w = 7–14 mm), with the exception of D16, whose mode is in the class of $d = 10$–20 mm. This distribution differs from that of the experimental products, which follows a decreasing exponential law. A comparison of the experimental and archaeological data highlights a marked deficit in artifacts smaller than 10 mm (Figure 13). This deficit is particularly important for the 2–4 mm class. Finally, we note that the ratio between the 20–31.5 mm class and that of the coarse pieces (> 31.5 mm) is approximately 1.6 times greater than the average value of the experiments. This difference also corresponds to a deficiency of coarse artifacts (Figure 14B).

The projection of values obtained at SD1 in a ternary diagram (Lenoble 2005; Bertran et al., 2006) shows that the archaeological series moves significantly away from the experimental values toward the coarse pole (Figure 14A).

Projections and Refitting

The distribution map of the lithics by raw material type reveals distinct concentrations (Figure 15A). Seven groups of conjoined pieces, each from a single block, can be distinguished, for which the refitting rate varies between 12.5 and 24%. However, this rate drops to 3% when considering all lithics greater than 2 cm. This overall rate, however, should be considered as a minimum because the refitting was not performed systematically.

The distribution map of all the lithic remains shows that the concentration of the artifacts varies in space, with areas poor in artifacts alternating with areas that are very rich (Figure 12). These form bands with an orientation of N 70°. On vertical projection AB (Figure 15B), the lithics form a ripple, the steepest face of which dips toward the south-southeast. The height of this ripple is approximately 10 cm, and it exhibits well-defined internal cross bedding. Group 1 of conjoined artifacts is characterized by a vertical and horizontal concentration of pieces over the gently sloping ripple face. In the more southwesterly squares, some pieces of this same group are scattered over the entire thickness of the archaeological layer. On projection CD (Figure 15B), oriented at 90° to the previous projection, the artifacts are arranged in horizontal beds. Group 2 is found in the lower portion of the archaeological level in an easily identifiable bed and is

Figure 10 View of the archaeological level during excavation.

Table III Proportions of the main technological categories within the SD1 lithic assemblage.

All materials—$n = 5488$	%
Cores	0.7
Blades	15.5
Pointed flakes	13.0
Levallois flakes	5.6
Cortical flakes	18.3
Undifferentiated flakes	35.1
Debris/fragments	11.4
Pebbles/worked pebbles	0.4

covered by another bed of artifacts. Group 4 is uppermost in the stratigraphy in a subhorizontal position and not covered by other artifacts.

Faunal Remains

The site excavation yielded 97 faunal remains, the vast majority of which ($n = 64$) were too fragmentary for precise taxonomic determination. All of the identified faunal remains correspond to dental fragments of mammalian herbivores and omnivores: Equidae ($n = 9$); Bovidae (*Caprinae*, $n = 12$); Hystricidae (*Hystrix* sp. cf. *H. indica*, $n = 3$); and Suidae (*Sus scrofa*, $n = 9$). The Equidae remains are attributed to *Equus sp. cf. Equus hemionus*, a species currently confined to Asian steppe and desert environments (Reading et al., 2001) but previously unreported in the Arabian Peninsula. The preservation status of the bone fragments is generally very poor. The absence of identifiable cutmarks on the fragments, caused by their poor surface preservation, prevents confirmation that their accumulation was solely anthropogenic. All of the collected faunal remains are small (< 5 cm in length), and more than half correspond to tooth fragments (55.2% of the bone material). The rest are compact bone fragments. The distribution of the faunal remains does not form any particular concentration and is distributed along the ripples in a manner comparable to that of the lithics.

DISCUSSION

Paleoenvironments

The archaeological site of SD1 results from a human occupation on an alluvial plain that was subject to periodic flooding. The combination of low C:N ratio and –21‰ mean $\delta^{13}C$ for the organic matter shows that it mostly derived from algae (Meyers, 1994), and suggests the persistence of at least seasonal water pools in the wadi. The lack of soil horizons implies a significant accretion rate of the floodplain and/or environmental conditions that were unfavorable to the development of vegetation. The chronological framework obtained by OSL shows that the accretion rate of the plain by flood deposits was high,

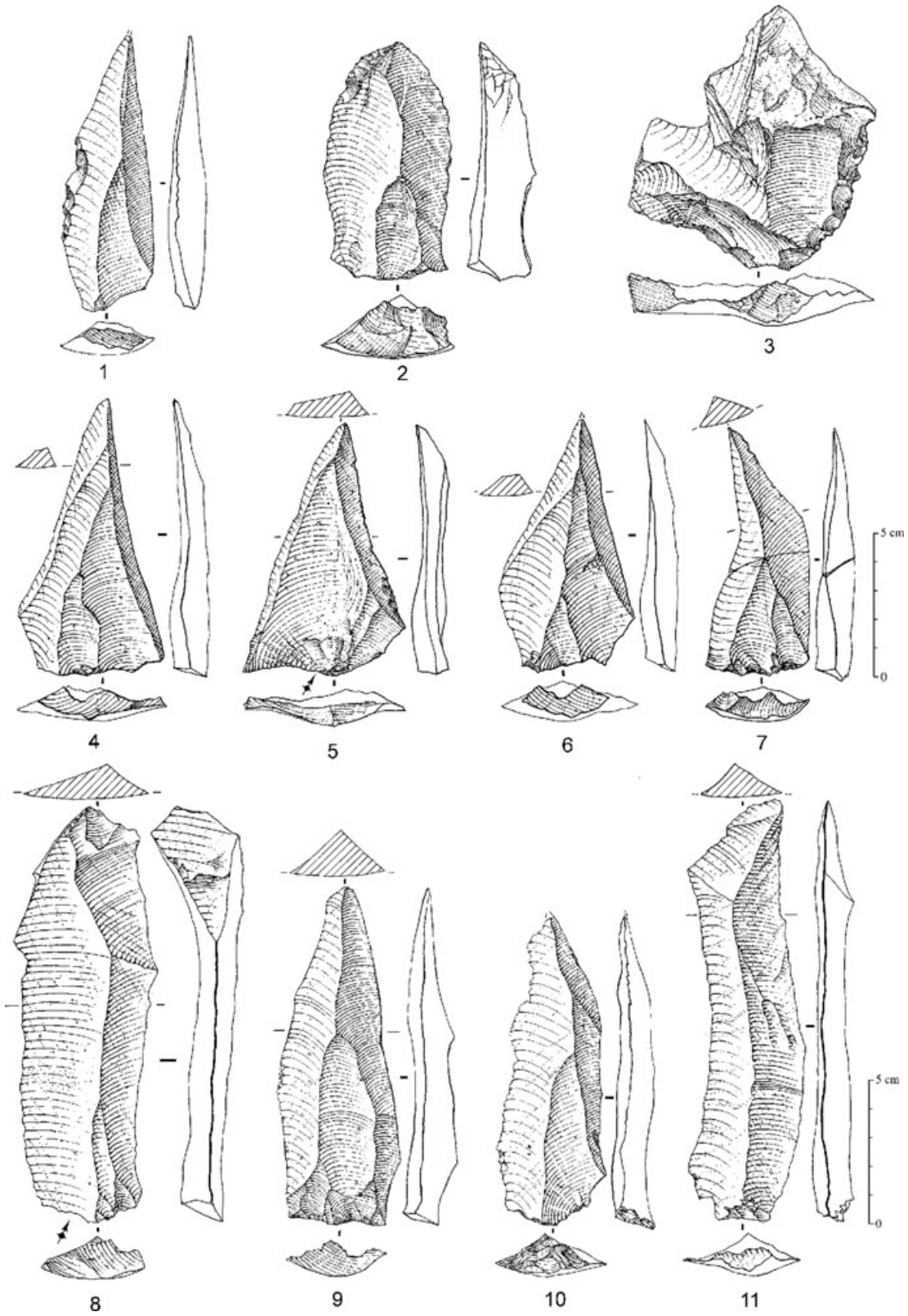

Figure 11 Main types of tools and lithic products of the SD1 assemblage: 1, 3—denticulated tools, 2—atypical endscraper, 4–7—pointed flakes, 8 to 11 – blades (Drawings by Jacques Jaubert).

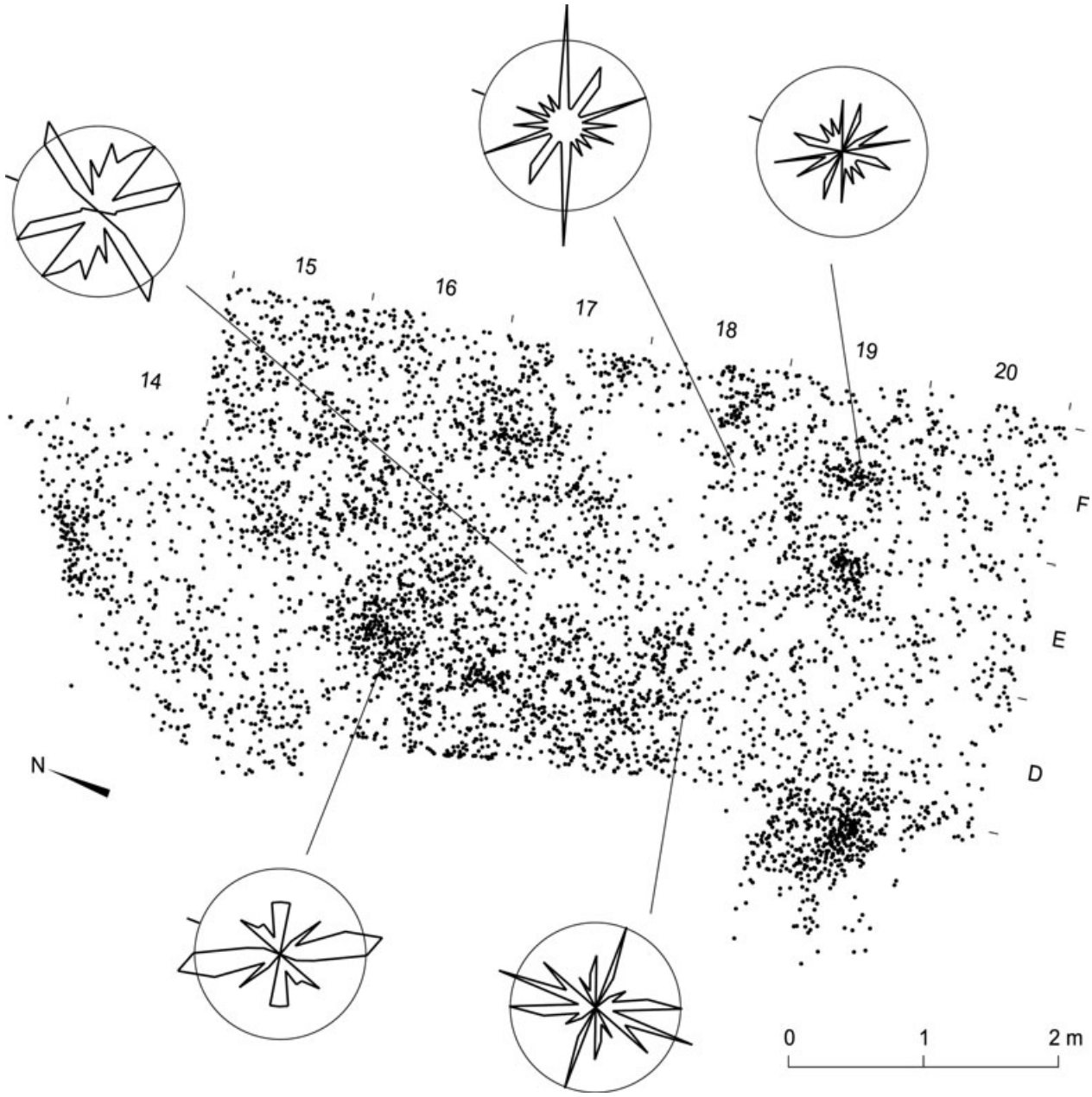

Figure 12 Spatial distribution of the SD1 remains and rose diagrams of the orientation of the elongated artifacts.

with all 30 m of the Shi'Bat Dihya Member revealing OSL ages ranging from 63 to 42 ka. Massive inputs of loess on the Great Escarpment and the piedmont downwind from the dune fields of the coastal plain and its redistribution by rivers may account for this rapid accretion rate. Such a configuration (a sprawling sandy plain with loess on the surrounding topography) is a common feature of eolian environments (Pye, 1995; Masson et al., 1999). Other more distant sources of loess such as the Rub' al Khali desert in the Arabian Peninsula (Crouvi et al., 2010) or East Africa (Middleton and Goudie, 2001) are also possibly involved. Data from Leuschner and Sirocko (2003) on cores taken in the Arabian Sea and those of Preusser (2009) on the Wahiba Sands of the Arabian Peninsula show a major peak input of dust and the establishment of sand dunes during the period preceding the deposit of the Shi'Bat Dihya Member, that is, approximately during MIS 4 (Figure 16). These aeolian deposits primarily fed the alluvial sedimentation in a pattern similar to that described in Namibia (Eitel et al., 2001). It is also

Table IV Statistical parameters.

	N	L1 (%)	L2 (%)	p (L1)	p (L2)	E1	E2	E3	IS	EL
D18	41	13.449	25.628	0.476	0.068	0.584	0.407	0.009	0.015	0.303
D16	46	15.861	9.639	0.298	0.652	0.529	0.459	0.012	0.022	0.133
E16	37	12.595	25.279	0.247	0.053	0.556	0.431	0.013	0.024	0.224
F 17-F18	40	16.297	11.839	0.190	0.525	0.538	0.449	0.013	0.024	0.166
Total	228	3.755	12.886	0.725	0.023	0.510	0.478	0.013	0.026	0.063

N, number of measurements; L, Vector Magnitude (Curray, 1956); E1, E2, E3, normalized eigenvalues; IS, isotropy index (IS = E3/E1); EL, elongation index (EL = 1 – (E2/E1)) according to Benn (1994).

probable that the dominant role played by hyperconcentrated flood flows in the upper part of the stratigraphy is a consequence of increased input of dust by wind during the alluvial sedimentation.

The presence of secondary gypsum crystals in the pores and of groundwater calcrete, however, indicates conditions of water balance deficit and high evaporation that occurred at least seasonally. These relatively arid conditions, consistent with the information provided by the fauna, do not correspond to the driest periods of the last climatic cycle reported for the Arabian Peninsula. The chronological data show that these alluvial formations were established during MIS 5 (Al Sharj Member) and at the beginning of MIS 3 (Shi'Bat Dihya Member), which correspond to phases of reinforcement of the influence of the summer monsoon (Clemens and Prell, 2003; Leuschner and Sirocko, 2003; Figure 16). MIS 4 and 2 have left no identifiable sedimentary record within the area investigated so far and were likely marked by a cessation of the alluvial sedimentation as a result of hyperaridity, which was mainly associated with aeolian dynamics and the formation of desert pavements. In contrast, the phases of basin incision separating the different sedimentary members correspond to periods of very high water flux in the wadis (*cf*. Lane, 1955; Eitel et al., 2001) in conjunction with the major peaks of humidity identified on the peninsula during the MIS 5e, 5c, 5a, and the beginning of the Holocene (Fleitmann and Matter, 2009; Fleitmann et al., 2011; Rosenberg et al., 2011).

Formation of the Archaeological Level

Several convergent taphonomic arguments lead to the conclusion that the site of SD1 has a complex history and has undergone significant transformations by fluvial activity. First, the particle size analysis of lithics suggests a truncated assemblage with a composition that is significantly different from the initial composition. Compared with what would be expected from a site where knapping activities took place (Schick, 1986; Bertran et al., 2006), this distortion is characterized by the underrepresentation of artifacts of both the small (d < 10 mm) and the large (d > 31.5 mm) classes. All stages of tool production are represented at SD1, testifying to *in situ* rhyolite knapping. The best hypothesis to explain the relative paucity of small pieces, which were waste products and therefore unlikely to have been of interest to the Paleolithic toolmakers (either to import or export), is the effect of hydraulic sorting of the lithic assemblage during the flooding of the wadi. Compared with the experimental data of Schick (1986) in ephemeral rivers of Africa, the bell shape of the particle size distribution indicates that artifact transport is accompanied by the selection of a particular dimensional class as a function of the power of the flow and the distance of transport. This transport likely affected the representation of the different categories of artifacts in the assemblage. Delagnes et al. (2012) find a deficiency in cores and in large cortical flakes derived from the initial phases of exploitation of the raw material. This deficit could be understood, at least in part, as a result of hydraulic sorting, with large and low-mobility pieces dropped upstream by the flows.

The spatial analysis of the SD1 archaeological level highlights a nonhomogenous distribution of the lithic artifacts, which results in concentrations in the form of parallel bands with internal, oblique bedding in cross-section and horizontal bedding in frontal section. This organization is interpreted as current ripples with slightly sinuous crests (Reineck and Singh, 1975). These ripples typically form under the influence of slow to moderate currents (0.1–1 m/s) and are common on the bottom of secondary channels, at the top of sand bars, or in the floodplains of rivers. No comparable feature was identified elsewhere in the floodplain deposits of the Shi'Bat Dihya Member. It is thus possible that the spots of artifacts, abandoned on a sandy silt surface, have themselves created the hydrodynamic conditions necessary for the development of current ripples, causing a local reduction in the thickness of the water layer and a subsequent increase in the speed of the flows.

Fabric measurements performed in different squares of the archaeological level have revealed two main preferred orientations: the N 60–70° direction, which is parallel to the crest of the artifact ripples, and the

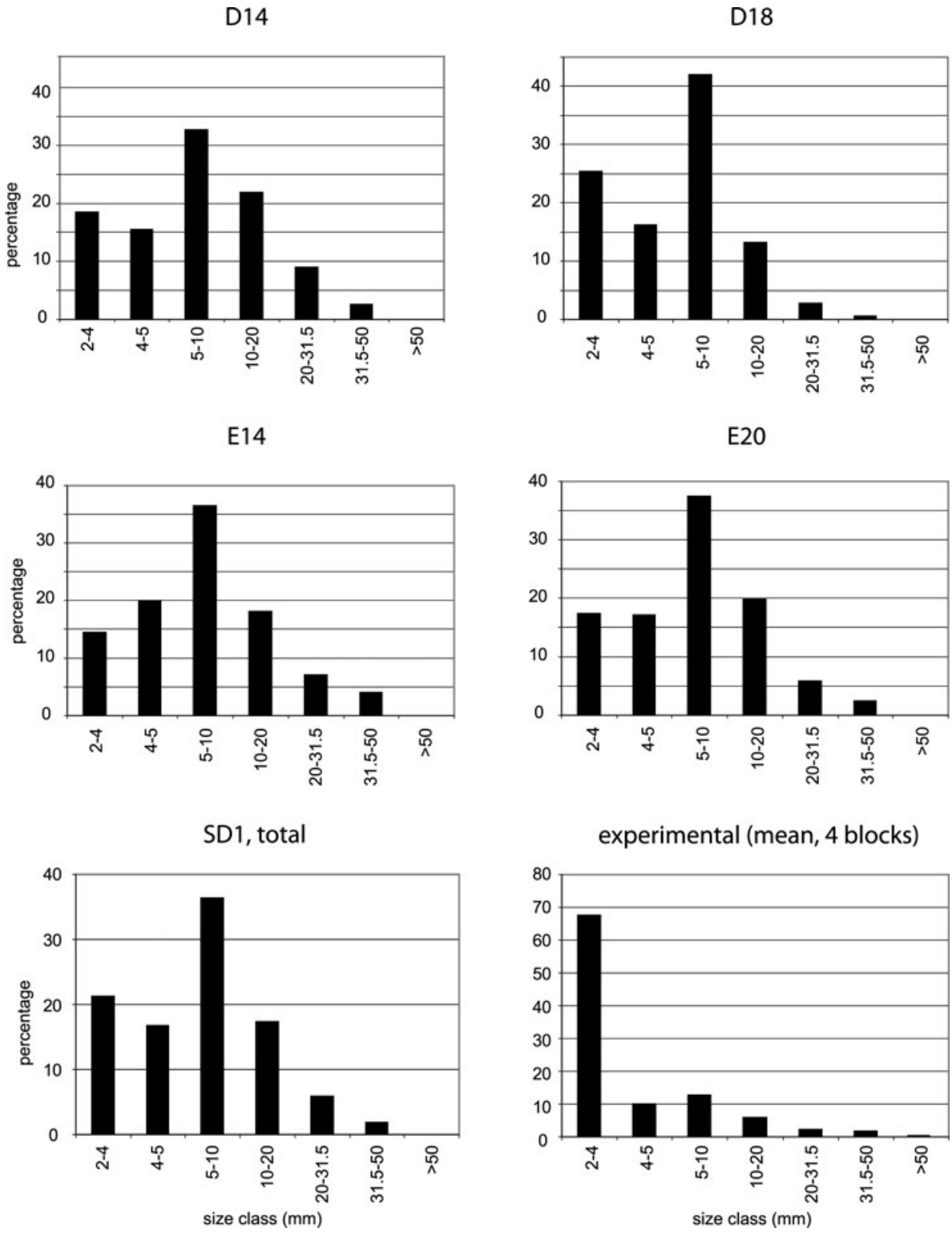

Figure 13 Comparative particle size of the experimental debitage and the archaeological layer.

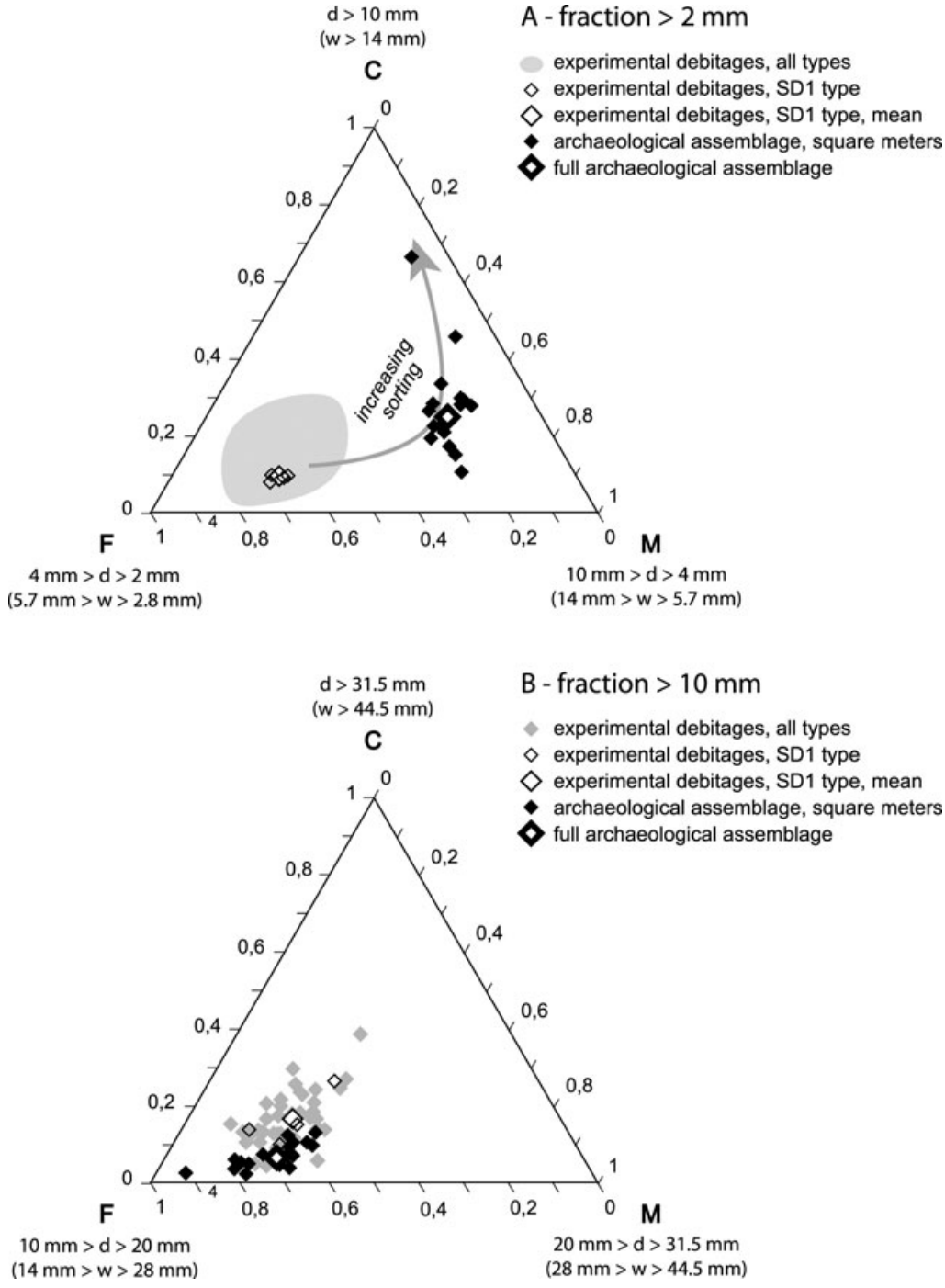

Figure 14 Particle size of the lithic material, triangular diagrams. (A) Fraction greater than $d = 2$ mm; the changing composition in relation to hydraulic sorting is indicated according to Lenoble (2005). (B) Fraction greater than $d = 10$ mm.

N 140–180° direction, approximately perpendicular to this crest. The bimodal orientation of the pebbles is characteristic of alluvial beds (Sedimentary Petrology Seminar, 1965; Rust, 1972). The most stable positions for pebbles subjected to shear stress exerted by flow on the river bottom are in effect either a parallel arrangement to the current or a transverse arrangement, which is usually accompanied by a marked imbrication. Rapid changes in

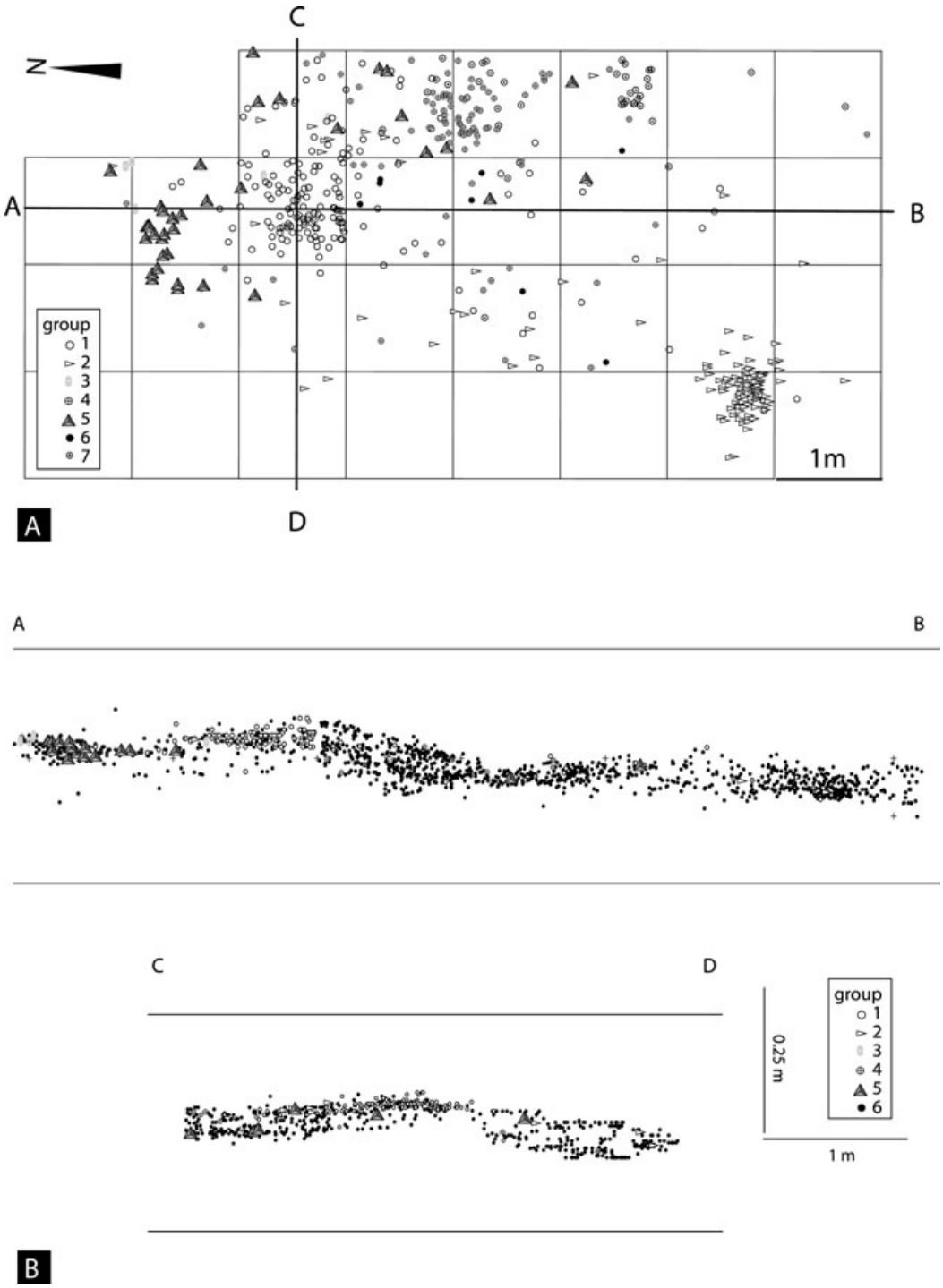

Figure 15 (A) Spatial distribution of products from seven refitted rhyolite blocks, and location of vertical projections. (B) Vertical projections of the archaeological material. The vertical scale has been doubled. The location of the projections is shown in Figure 15(A).

direction are also frequently reported on the same pebble bar and reflect fluctuations in the direction of water streams according to the local topography. This type of fabric was also found, albeit not systematically, in Schick's experiments (1986). Two factors may be invoked to explain the variability observed at SD1. First, the water flow was shallow, and the topography corresponding to the accumulation of artifacts displaced the local flow

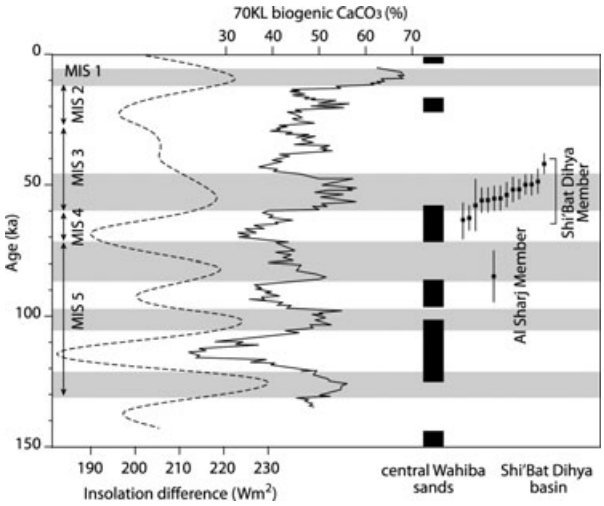

Figure 16 Chronology of the Shi'Bat Dihya and Al Sharj Members compared with the emplacement of the Wahiba Sands of Oman (according to Preusser, 2009) and with summer monsoon fluctuations over the peninsula (core 70 KL, according to Leuschner and Sirocko, 2003). The content of biogenic $CaCO_3$ in core 70KL (maxima shaded in gray) is inversely correlated with the contribution of dust in the Arabian Sea; the curve of the summer insolation difference between 30°S and 30°N is a measure of the intensity of the Indian monsoon (Leuschner and Sirocko, 2003). This points to the development of Shi'Bat Dihya and Al Sharj Members during moderate monsoon reinforcement phases.

directions (e.g., see Miall, 1996). Second, the orientation of the artifacts was not homogenous throughout the thickness of the archaeological layer, and the measurements are influenced by the relative importance of each sublevel.

Several arguments suggest that the concentrations of the conjoined pieces do not correspond to *in situ* knapping spots but rather to secondary concentrations originating from the redistribution of knapping spots.

In particular,

1. the groups of conjoined pieces form thin beds within the archaeological layer, which are either localized at the base of the hydraulic ripples or at the top. This bedding is of fluvial origin.
2. the refitting rates calculated within these groups are low, between 12 and 24%. Pieces belonging to other blocks of raw material are also mixed with these concentrations.

This interpretation can be related to the observations made by Schick (1986) in one of her experimental cells. This author has shown that pieces that belonged to the same initial concentration could be found close to each other in secondary clusters after a brief transit along the riverbed. The transport was accompanied by a depletion of small elements and the reorientation of the artifacts perpendicular to the direction of flow.

Our results point to the following scheme for the formation of the site, which consisted of three main phases:

1. Lithic artifacts were abandoned by the occupants of the site on a floodplain. The strictly anthropogenic origin of the bones associated with the lithic artifacts cannot be proven because they were poorly preserved. However, an anthropogenic origin is considered to be very likely because no piece of bone was found in the stratigraphic sequence outside of the archaeological layers discovered in the Shi'Bat Dihya Member.
2. Flood flows moved and reorganized the lithics in the form of current ripples. This transport was accompanied by a particle size sorting: the smallest elements were carried farther downstream, whereas larger elements, which are less mobile, remained closer to the original site location upstream of the excavated area. It seems likely that the scarcity of faunal remains and the absence of large pieces of bone is a result of hydraulic sorting in addition to the role played by weathering. Indeed, the bones have a lower density compared to the lithic materials, whereas their thickness (and their susceptibility to being carried by a current) is on average higher. The overrepresentation of dental remains (more than half of the faunal assemblage), the density and morphology of which are more similar to those of the rhyolite artifacts, should also partly reflect the action of the current. This type of faunal assemblage is similar to that described as 'lag deposit' by Voorhies (1969) and Behrensmeyer (1976) in the context of channels or floodplains.
3. The accretion of the floodplain continued, and the site was rapidly covered by sand and silt from flood flows, as suggested by the nearly absence of traces of pedogenesis and by the homogenous ages obtained over the entire alluvial sequence. The short-term exposure of the archaeological layer to the action of floods likely explains the persistence of a relic anthropogenic organization, indicated by the concentrations of conjoined pieces, the local non-negligible refitting rate, and the almost lack of visible abrasion of the pieces. From a geological point of view, the lithic assemblage may be considered "in place," that is, subcontemporary to the alluvial deposits in which it is interstratified. As a consequence, OSL dates obtained from alluvial deposits provide a good estimation of the age of the human activity at the site.

CONCLUSIONS

The site of SD1 (western Yemen) corresponds to a Middle Paleolithic occupation in the floodplain of Wadi Surdud at the beginning of MIS 3. This floodplain was subject to rapid accretion as a consequence of intense remobilization of loess deposited on the piedmont and the Great Escarpment of Yemen. The pedological data indicate relatively dry conditions during the occupation of the site, which was marked by a high evaporation rate, leading to the formation of gypsum and calcretes. These conditions indicate the adaptation of the local human groups to (semi)-desert environments. However, according to the data derived from marine cores (Clemens and Prell, 2003; Leuschner and Sirocko, 2003), these conditions do not correspond with the driest phases of the last climatic cycle but rather with periods of enhanced summer monsoon and relative increase in humidity at a regional scale.

The results of the taphonomic study conducted on the SD1 level confirm that even in a floodplain environment usually considered to be very favorable for site preservation, the archaeological record can be significantly altered by geomorphological processes. The degradation, related to the flooding of the wadi, has implications for the archaeological interpretation of the occupation level investigated so far. Indeed, the spatial distribution of the artifacts at SD1 cannot be considered to be only of anthropogenic origin but also reflects the action of flows. A particle size sorting has also occurred, and the underrepresentation of certain categories of artifacts (small-sized debris and large pieces such as cores) does not result from human export but rather from hydraulic transport. Hydraulic sorting has also affected the distribution and likely the representativeness of the faunal materials.

As a whole, this case study shows that detailed geoarchaeological investigations are necessary in any environment to appropriately assess the quality of information provided by the archaeological layer and to identify the possible biases and distortions in the interpretation of the assemblages. In fact, the validity of the spatial distribution analysis of the artifacts to identify the organization of human activities within an archaeological site is highly dependent on secondary modifications by geomorphological processes. Similarly, the interpretation of the economic status of a site, partly based on the analysis of the relative proportions of different categories of lithic products, needs to be validated that no further sorting of the remains occurred. Even if these two conditions are not fulfilled as in the case of the SD1 site, the study nonetheless indicates that the homogeneity and the "in place" geological character of the assemblage grant its potential informative value for the comprehension of the technological strategies of the Middle Paleolithic people who settled in Wadi Surdud.

The Paleo-Y international paleoanthropological research project, developed since 2005 by R.M. in agreement with the Yemeni General Organization for Antiquities and Museums (GOAM) and the Centre Français d'Archéologie et de Sciences Sociales de Sanaa (CEFAS), has been granted by the French Ministry of Foreign Affairs (to R.M.), the French CNRS project Eclipse II (to R.M.), the L.S.B. Leakey Foundation (to A.D.). Paleo-Y, whose action was initiated by the generous help of A. de Maigret (University of Naples) and J.-F. Jarrige (CNRS), greatly benefited from the support of the University Bordeaux 1 (UMR PACEA CNRS), the University of Poitiers (Department of Geosciences), and the French Institut National de Recherches Archéologiques Préventives (INRAP), and also from the collaboration of the French Muséum National d'Histoire Naturelle and the University "La Sapienza" of Rome. For research permission and collaboration, Paleo-Y is indebted to A. Ba-Wazir, General Director of the GOAM; A. Garallah, Deputy of the GOAM; and A.A. Mohsen, Governor of Al-Mahqwid. We acknowledge the extraordinary continuous support provided by J. Lambert and M. Tuchscherer, directors of the CEFAS. The archaeological excavations at SD1 and SD2 have been realized under the scientific direction of A.D. and J.J., respectively. In addition to the authors of this study, the Paleo-Y field work in Tihama and the specific research at Wadi Surdud have been also contributed by E. Abbate, N. Abdulbaset, A. Abraudey, K. Al-Haj, M. Al-Halabi, A.S. Alrudy, A. Ballah, A. Coppa, A. Mosabi, H. Murad, M.A. Qasam, C. Thiébaut, J.-F. Tournepiche, P. Voinchet, and have received the friendly support of E.H. Awadh, A.M. Farea, I. Hehmeyer, and E. Keall, of the Granary's Museum of Zabid, and of M.A. Al-Sayyani and M. Rajeh Murad, of the GOAM. M.-C. Noël and H. Goubar, respectively, assured most of the administrative and logistical aspects during the missions in Yemen. With special reference to the present study, we particularly thank S. Dubernet for the Raman analyses, H. Etcheber for the determination of TOC and $CaCO_3$, V. Eisenman for the determination of the equine remains, and A. Lenoble for bibliographic assistance. We are sincerely obliged to the people of the Al-Mahqwid and Tihama regions for their welcome and interest in our research activities and acknowledge the support of A. Auotnan, representative of the District of Khamis Bani Saad. J. Woodward and two anonymous reviewers are also acknowledged for their helpful critical review of the manuscript.

REFERENCES

Allmendinger, R.W. (2005). Stereonet 6.3.3. http://www.geo.cornell.edu/geology/faculty/

Behrensmeyer, A.K. (1976). Fossil assemblages in relation to sedimentary environments in the East Rudolf Succession. In Y. Coppens, C. Howell, G. Isaac & R. Leakey (Eds.), Earliest man and environments in the Lake Rudolf Basin (pp. 383–401). Chicago: University of Chicago Press.

Benn, D.I. (1994). Fabric shape and the interpretation of sedimentary fabric data. Journal of Sedimentary Research, 64, 910–915.

Bertran, P., & Texier, J.-P. (1995). Fabric analysis: application to paleolithic sites. Journal of Archaeological Science, 22, 521–535.

Bertran, P., Claud E., Detrain L., Lenoble, A., Bertrand, M., & Vallin, L. (2006). Composition granulométrique des assemblages lithiques, application à l'étude taphonomique des sites paléolithiques. Paleo, 18, 1–30.

Clemens, S.C., & Prell, W.L. (2003). A 350,000 year summer-monsoon multi-proxy stack from the Owen Ridge, northern Arabian Sea. Marine Geology, 201, 35–51.

Courty, M.A., & Fédoroff, N. (1985). Micromorphology of recent and buried soils in a semi-arid region of Northwest India. Geoderma, 35, 287–332.

Crouvi, O., Amit, R., Enzel, Y., & Gillespie, A.R. (2010). Active sand seas and the formation of desert loess. Quaternary Science Reviews, 29, 2087–2098.

Curray, J.R. (1956). The analysis of two-dimensional orientation data. Journal of Geology, 64, 117–131.

Delagnes, A., Tribolo, C., Bertran, P., Brenet, M., Crassard, R., Jaubert, J., Khalidi, L., Mercier, N., Nomade, S., Peigné, S., Sitzia, L., Tournepiche, J.F., & Macchiarelli, R. (2012). Inland human settlement in southern Arabia 55,000 years ago. New evidence from the Wadi Surdud Middle Paleolithic site complex, western Yemen. Journal of Human Evolution, 63, 452–474.

Downs, R.T. (2006). The RRUFF Project: an integrated study of the chemistry, crystallography, Raman and infrared spectroscopy of minerals. Program and Abstracts of the 19th General Meeting of the International Mineralogical Association in Kobe, Japan, July 23–28, 2006.

Eitel, B., Blümel, W.D., Hüser, K., & Mauz B. (2001). Dust and loessic alluvial deposits in Northwestern Namibia (Namaraland, Kaokoveld): Sedimentology and palaeoclimatic evidence based on luminescence data. Quaternary International, 76–77, 57–65.

Fleitmann, D., & Matter, A. (2009). The speleothem record of climate variability in Southern Arabia. C.R. Geoscience, 341, 633–642.

Fleitmann, D., Burns, S. J., Pekala, M., Mangini, A., Al-Subbary, A., Al-Aowah, M., Kramers, J., & Matter, A. (2011). Holocene and Pleistocene pluvial periods in Yemen, southern Arabia. Quaternary Science Reviews, 30(7–8), 783–787.

Galbraith, R.F., & Green, P.F. (1990). Estimating the component ages in a finite mixture. Nuclear Tracks and Radiocarbon Measurements, 17, 197–206.

Gauthier, C., & Hatté, C. (2008). Effects of handling, storage, and chemical treatments on delta C-13 values of terrestrial fossil organic matter. Geophysics, Geochemistry and Geosystem, 9, Q08011, doi:10.1029/2008GC001967.

Guilloré, P. (1980). Méthode de fabrication mécanique et en série des lames minces. Unpublished report. Paris-Grignon, Institut National d'Agronomie, 22 p.

Lane, E.W. (1955). The importance of fluvial morphology in hydraulic engineering. Proceedings of the American Society of Civil Engineers, 81 (745), 1–17.

Lanson, B. (1997). Decomposition of experimental X-ray diffraction patterns (profile fitting): A convenient way to study clay minerals. Clays and Clay Minerals, 45, 132–146.

Lenoble, A. (2005). Ruissellement et formation des sites préhistoriques : référentiel actualiste et exemples d'application au fossile. BAR International Series, 1363. Oxford: British Archaeological Reports.

Lenoble, A., & Bertran, P. (2004). Fabric of Palaeolithic levels: Methods and implications for site formation processes. Journal of Archaeological Science, 31, 457–469.

Leuschner, D.C., & Sirocko, H. (2003). Orbital insolation forcing for the Indian monsoon – A motor for global climate changes? Palaeogeography, Palaeoclimatology, Palaeoecology, 197, 83–95.

Li, W., Qi, P., & Sun, Z. (1997). Deformation of river bed and the characteristics of sediment transport during hyper-concentrated flood in the Yellow River. International Journal of Sediment Research, 12(3), 72–79.

Macchiarelli, R. (2009). From Africa to Asia through Arabia: models, predictions, and witnesses of first phases of human settlement. In: O. Suleimenov & W. Iwamoto (Eds.), First great migrations of peoples (pp. 19–25). Paris: UNESCO.

Macchiarelli, R., & Peigné, S. (2006). Le premier peuplement de l'Arabie méridionale: la perspective Tihama (Yémen). Bulletin et Mémoires de la Société d'Anthropologie de Paris, 18, 231. (Abstract)

Mack, G.H., David, R.C., & Treviño, L. (2000). The distribution and discrimination of shallow, authigenic carbonate in the Pliocene-Pleistocene Palomas Basin, southern Rio Grande rift. Geological Society of American Bulletin, 122, 643–656.

Masson, J.A., Nater, E.A., Zanner, C.W., & Bell, J.C. (1999). A new model of topographic effects on the distribution of loess. Geomorphology, 28, 233–236.

Meyers P.A. (1994). Preservation of elemental and isotopic source identification of sedimentary organic matter. Chemical Geology, 114, 289–302.

Miall, A.D. (1996). The geology of fluvial deposits. New York: Springer.

Middleton, M.J., & Goudie, A.S. (2001). Saharan dust: sources and trajectories. Transactions of the Institute of British Geographers NS, 26, 165–181.

Munro, R.N., & Wilkinson, T.J. (2007). Environment, landscape and archaeology of the Yemeni Tihamah. In J. Starkey, P. Starkey & T. Wilkinson (Eds.), Natural resources and cultural connections of the Red sea, BAR international series, (pp.13–33), S1661, Oxford: Arch.

Pierson, T.C., & Costa, J.E. (1987). A rheologic classification of subaerial sediment-water flows. In J.E. Costa & G.F. Wieczorek (Eds.), Debris flows/avalanches: Process, recognition and mitigation. Boulder, CO: Geological Society of America.

Porta, J., & Herrero, J. (1990). Micromorphology and genesis of soils enriched with Gypsum. In L.A. Douglas (Ed.), Soil

micromorphology: a basic and applied science, developments in soil science 19, (pp.321–339). Amsterdam: Elsevier.

Preusser, F. (2009). Chronology of the impact of Quaternary climate change on continental environments in the Arabian Peninsula. C.R. Geoscience, 341, 621–632.

Pye, K. (1995). The nature, origin and accumulation of loess. Quaternary Science Reviews, 14, 653–667.

Reading, R.P., Mix, H.M., Lhagvasuren, B., Feh, C., Kane, D.P., Dulamtseren, S., & Enkhbold, S. (2001). Status and distribution of khulan (Equus hemionus) in Mongolia. Journal of Zoology, 254, 381–389.

Reineck, H.-E., & Singh, I.B. (1975). Depositional sedimentary environments. Heidelberg, Germany: Springer-Verlag, Berlin.

Reynolds, R.C. (1985). NEWMOD, a computer program for the calculation of one-dimensional diffraction patterns of mixed-layer clays. In R. C. Reynolds Jr. & Dr. Brook (Eds.), Hanover, New Hampshire.

Rosenberg, T. M, Preusser, F., Fleitmann, D., Schwalb, A., Penkman, K., Schmid, T. W., Al-Shanti, M. A., Kadi, K., & Matter, A. (2011). Humid periods in southern Arabia: Windows of opportunity for modern human dispersal. Geology, 39(12), 1115–1118.

Rust, B.R. (1972). Pebble orientation in fluvial sediments. Journal of Sedimentary Petrology, 42, 384–388.

Schick, K.D. (1986). Stone Age sites in the making. Experiments in the formation and transformation of archaeological occurrences. BAR International Series 319, Oxford: British Archaeological Reports.

Sedimentary Petrology Seminar. (1965). Gravel fabric in Wolf run. Sedimentology, 4, 273–283.

Valentin, C., & Bresson, L.-M. (1992). Morphology, genesis and classification of surface crusts in loamy and sandy soils. Geoderma, 55, 225–245.

Voorhies, M.R. (1969). Taphonomy and population dynamics of an early Pliocene vertebrate fauna, Knox County, Nebraska. Contributions to Geology, Special Paper no. 1. Laramie, Wyoming: University of Wyoming.

Wright, V.P. (2007). Calcrete. In D.J. Nash and S.J. McLaren (Eds.), Geochemical sediments and landscapes (pp. 10–45). Oxford: Blakwell Science.

Xu, J. (1998). A study of physico-geographical factors for formation of hyperconcentrated flows in the loess plateau of China. Geomorphology, 24, 245–255.

